Open Access

*Advances in Environmental and Engineering Research*

LIDSEN Publishing Inc.

Original Research

# The Remediation of Hexavalent Chromium Using Orange Peel Biosorbent from Industrial Effluents

Muhammad Kashif Channa [1], Muhammad Waris [2, *], Sultana Rahman [3], Ali Bahar Shahani [4]

1. National Centre of Excellence in Analytical Chemistry, University of Sindh Jamshoro Sindh, Jamshoro, Pakistan; E-Mail: mkchanna18@gmail.com
2. Department of Environmental Science, Aror University of Art, Architecture, Design and Heritage, Sukkur Sindh Pakistan; E-Mails: mwaris.faculty@aror.edu.pk; warisarain90@gmail.com
3. Department of Chemistry, Quaid-I-Azam University, Islamabad, Pakistan; E-Mail: sultana.rahman@chem.qau.edu.pk
4. Department of chemistry, Shah Abdul Latif University, Khairpur, Pakistan; E-Mail: Ali.bahar26@yahoo.com

* **Correspondence:** Muhammad Waris; E-Mails: mwaris.faculty@aror.edu.pk; warisarain90@gmail.com

**Academic Editor:** Mohammad Boshir Ahmed

**Special Issue**: Advanced Materials and Technologies for Pollutants Removal and Environmental Remediation

*Adv Environ Eng Res*
2025, volume 6, issue 1
doi:10.21926/aeer.2501011

**Received:** February 28, 2024
**Accepted:** December 12, 2024
**Published:** February 09, 2025

**Abstract**

One major cause of aquatic pollution is the accumulation of heavy metal ions. This study shows the biosorption properties of orange peel for removing chromium ($Cr^{VI}$) from industrial wastewater at a laboratory scale. This study focused on the biosorption of $Cr^{VI}$ using orange peel biosorbent (OPB) from aqueous solutions in the plastic industry (PI), textile and fabrics industry (TFI), chemical industry (CI), and food industry (FI). The total Cr contents in effluents of FI, CI, TFI and PI varied between 30.0-38.0, 23.0-27.0, 35.0-95.0 and 40.0-180 mg $L^{-1}$, respectively. Understanding the physical and chemical characteristics of $Cr^{VI}$ is necessary for successful bioremediation using OPB. The $Cr^{VI}$ is bound to OPB (the peel of *Citrus aurantium*)

© 2024 by the author. This is an open access article distributed under the conditions of the Creative Commons by Attribution License, which permits unrestricted use, distribution, and reproduction in any medium or format, provided the original work is correctly cited.

by interactions with the biomass's amine and -CO functional group, according to the FT-IR spectra. The change in morphology of OPB was checked by scanning electron microscopy (SEM) after loading of $Cr^{VI,}$ indicating that the bio-sorption of $Cr^{VI}$ occurs on the OPB. From water samples at an ideal pH of 7, a contact period of 20 min, and a temperature of 298 K, the $Cr^{VI}$ biosorption capacity of the biosorbent material was reported to be 0.222 mmol/g (48.0 mg/g). The results show that OPB can be used as an adsorbent or stabilizer for $Cr^{VI}$ from industrial effluents.

**Keywords**
Remediation; chromium (VI); orange peel biosorbent; industrial effluent

## 1. Introduction

Natural water often contains chromium in the oxidation states of trivalent ($Cr^{III}$) and hexavalent ($Cr^{VI}$). Chromium in the oxidation states of trivalent ($Cr^{III}$) and hexavalent ($Cr^{VI}$) is frequently found in natural water. These can vary greatly from one another because of their unique biological, geochemical, and toxicological characteristics [1]. $Cr^{III}$ compounds are sparingly soluble in water, while $Cr^{VI}$ compounds are readily soluble to enhance the levels of $Cr^{VI}$ in water sources. Humans can be exposed to Cr, when eating food, drinking water and inhaling air [2]. The average daily intake of total Cr from air, water, and food is estimated to be 0.01-0.03 mg, 2.0 mg $L^{-1}$, and 60 mg, respectively. Trivalent chromium ($Cr^{III}$) is an essential mineral for maintaining optimal glucose tolerance, lipid and protein metabolism, and other human metabolic functions [3]. The most hazardous type of Cr, however, is $Cr^{VI}$, due to it has strong oxidation potential, which allows it to permeate biological cell membranes and damage macromolecules, proteins, and DNA, it has some carcinogenic consequences [4, 5]. The $Cr^{VI}$ is damaging to the lungs, liver, and kidneys and inhibiting the cell's enzymatic uptake of sulphur. Chronic ulceration, dermatitis, a corrosive response in the nasal septum, and local lung damage are the main toxic consequences of $Cr^{VI}$ [6].

The metallurgical industry primarily uses the $Cr^{VI}$ compounds for chrome plating and chrome alloy. In the chemical industry, it serves as an oxidizing agent in the form of various Cr compounds. Different compounds of Cr are also used for tanning leather. As a result, about 40% of used Cr is discharged in the effluents as $Cr^{VI}$ [7]. The compounds $Cr^{VI}$ were also used in textile dyeing, ceramics, glass and photography. About 90% of chromium produced from chrome ore was used in metallurgical industries for steel, alloy, and nonferrous alloy production [8]. Whereas the remaining extracted chrome was used for the rest of the industrial activities. The untreated industrial and municipal wastes have created multiple environmental problems for mankind. Effluent discharge from the industries is a potential source of aquatic environmental pollution [9]. Industrial effluents can be characterized by different physical properties like dark colour, pH, suspended solids (SS), chemical oxygen demand (COD) and high biochemical oxygen demand (BOD). Elevated level of COD indicates the recalcitrance of discharged chemicals [10]. The chemicals present in water bodies may lead to bioaccumulation in both plant and animal's systems [10, 11]. Therefore, the gradual monitoring and assessment of Cr and its different forms in industrial effluents is very important [6, 12]. Ion exchange characteristics can be found in various natural and manmade goods. The most

significant ion exchangers are, by far, the organic resins. In order to remove $Cr^{VI}$ from synthetic wastewater, anion exchange resins are utilized. High chemical and mechanical stability, high ion exchange capacity, and high ion exchange rate are the key benefits of employing these resins [13]. Physical-chemical techniques such as ion exchange, precipitation, oxidation, and reverse osmosis have been used to remove $Cr^{VI}$ ions from industrial effluents [13, 14]. By reducing the $Cr^{VI}$ at an acidic pH and employing the proper lowering agents, the $Cr^{VI}$ has traditionally been removed from solutions [5, 15]. However, such technologies are expensive, and a large amount of sludge disposal may cause environmental problems. The key factors for implementing an effective remediation method are the cost and availability of adsorbent as well as the convenience of the treatment process.

Using raw orange peel, the adsorptions of numerous metal ions, including Pb(II), Ni(II), Zn(II), Cu(II), and Co(II), were investigated. When the orange peel is treated with nitric acid, the adsorption of these metals is 7.75, 6.01, 5.25, 3.65, and 1.82 mg/g, respectively [16]. The current study set out to use the natural biosorbent "orange peel" to remove $Cr^{VI}$ from industrial effluents. Utilizing orange peels with modifications to increase removal capacity will promote the process of treating industrial wastewater.

## 2. Materials and Methods

### *2.1 Sampling and Pretreatment*

#### 2.1.1 Industrial Effluent

Industrial effluents from several businesses in Jamshoro and Hyderabad were sampled at random. Based on their characteristics, the industries are grouped into four groups: the plastic industry (PI), the chemical industry (CI), the textile and apparel industry (TFI), and the food sector (FI). Each of the two or three industries that were selected for each category was represented by four samples (n = 40). In 1 L polyethylene plastic bottles, samples of industrial wastewater were collected. Half a portion was used for the BOD test using 500 ml size microbiological examination bottles, and the remaining portion was used for physical examination and speciation of chromium. The four quality indicators, such as pH, total dissolved solids (TDS), biochemical oxygen demand (BOD), and electric conductivity (EC), were then assessed for each sample.

#### 2.1.2 Biosorbent Collection and Pre-Treatment

The orange fruits were bought from a market in Hyderabad, Sindh, Pakistan, and the peel and pulp were separated. Following a series of washes with tap, distilled, and deionized water, the separated peels were allowed to air dry for a week. The peel was then pulverized and heated for two hours in an electric oven at 343 K. For the preparation of orange peel biosorbent (OPB), the dried material was ground and sieved in an electrical sieve shaker of the Ro-Tap type, and the US mesh No. 200 was used to collect the particles. Particles smaller than 100 µm were produced by sieving for the bio-sorption process. For future use, the sieved OPB was kept in a vacuum desiccator.

2.1.3 Chemicals and Reagents

The experiment used deionized water from an ELGA laboratory water system (Bucks, UK) with a resistance of 0.05 µs $cm^{-1}$. Analytical reagent-grade $HNO_3$ (purity 65%, Sp.gr: 1.41) and $H_2O_2$ (30%, Sp.gr: 1.11) were purchased from Merck (Darmstadt, Germany). Potassium dichromate ($K_2Cr_2O_7$; Sigma Chemical, MO, USA) (0.28 g) was dissolved in 1.0 L of 1.5% $HNO_3$ to prepare the 1000 mg $L^{-1}$ stock solution of $Cr^{VI}$. The certified standard solution was diluted to create the Cr standard solutions (1000 mg $L^{-1}$), Fluka (Buchs, Switzerland). The proper amount of 0.1 mol $L^{-1}$ HCl/NaOH solutions was added to adjust the solution's pH from 2 to 9. A pH meter was used to calibrate the pH of the solution. Acetone (Merck) was utilized directly without further purification. A minimal amount of acetone was used to dissolve 0.25 g of 1,5-diphenylcarbazide (Merk) and dilute it to 100 mL. The suitable dilution of concentrated sulfuric acid prepared sulfuric acid of the desired concentration. Before use, all glass and polyethylene bottles underwent a thorough cleaning, an overnight soak in 5 mol $L^{-1}$ $HNO_3$, and a thorough rinsing with distilled and deionized water.

### *2.2 Apparatus*

A pH meter was used to determine the samples' pH levels (781-pH meter, Metrohm). WIROWKA Laboratoryjna type WE-1, nr-6933 centrifuge (MechanikaPhecyzyjna, Poland) was used for centrifugation with speed ranging between 0-6000 rpm and timer 0-60 min. The samples were shaken using a flask electric shaker (Gallenkamp, England) 220/60 HZ. An agate ball mixer mill (MM-2000 Haan, Germany) ground the dry samples. For the quantitative examination of total Cr, inorganic Cr, and their species, a Perkin Elmer atomic absorption spectrometer, Model A Analyst 700 USA, with a deuterium lamp back corrector, pyro-coated graphite tubes with an integrated platform, and autosampler 800 is utilized [17]. The measuring condition of micro sample injection system-flame atomic absorption spectrometry (MIS-FAAS) and graphite furnace atomic absorption spectrometry (GFAAS) for $Cr^{VI}$ and total Cr were given in Table 1. The biosorption capability of the biosorbent was evaluated using an FTIR spectrometer and a scanning electron microscope (SEM) (JEOL model JSM-6380 and Thermo Nicolet Analytical Instruments, Madison, WI).

**Table 1** Measurement conditions for Cr by atomic absorption spectrometry (Hitachi 180-50 Japan).

| (a) Graphite furnace atomic absorption (GFAAS) | | | |
|---|---|---|---|
| | Cr | | |
| Lamp current (mA) | 7.5 | Dry[a] | 80-120/15 |
| Wave length (nm) | 357.9 | Ash[a] | 300-700/15 |
| Slit-width (nm) | 1.3 | Atomization[a] | 2600-2700/5 |
| Cuvette | Tube | Cleaning[a] | 2700-2900/2 |
| Chemical Modifier | $Mg(NO_3)_2$ | | |
| Carrier gas 200 ml/min and Sample volume 10 µl + 10 µl modifier in each case | | | |

| (b) Flame atomic absorption (FAAS) | | | | | |
|---|---|---|---|---|---|
| Elements | Wave length (nm) | Slit width (nm) | Lamp current (mA) | Burner height (mm) | Fuel (Acetylene kg $cm^{-2}$) |
| Cr | 357.9 | 1.3 | 7.5 | 7.5 | 0.35 |

$D_2$ Lamp used for background correction, Aspration rate (2 mL $min^{-1}$), [a]Temperature range°C/time(s), [b]air as an oxidant = 1.6 kg $cm^{-2}$.

### *2.3 Determination of $Cr^{VI}$*

The final volume was kept at 100 mL by adding 3.0 mL of 0.25% diphenylcarbazide after mixing 1.0 mL of a 10 mg $L^{-1}$ solution of $Cr^{VI}$ with 3.0 mL of 0.5 mol $L^{-1}$ $H_2SO_4$. 2 mL $min^{-1}$ of flow rate was kept up as the sample solution was placed onto the OPB-containing column. The absorbance of the resultant solution from the column demonstrated that the reddish violet complex was adsorbed onto the column. A subsequent step involved eluting the adsorbed compound with 15.0 mL of 2.5 M $H_2SO_4$ in acetone. To remove interference from organic matrices, the final solutions were evaporated to dryness at 80°C. The residues were diluted with 1.0 ml of 0.2 M $HNO_3$ solution. The concentration of $Cr^{VI}$ was determined by MIS-FAAS.

#### 2.3.1 Determination of Total Chromium

For total Cr, 100 mL of industrial effluent samples were filtered by Whatman No. 42 filter paper and pre-concentrated >25 mL at 70°C on an electric hot plate. Then, the resulting solution was kept at 4°C till further analysis, as described in previous work [18]. Analytical blanks were prepared similarly to samples but without the addition of a sample in order to determine the detection limit.

#### 2.3.2 Remediation of Cr Species

Batch equilibrium sorption experiments were carried out in 250 ml conical flasks with 100 ml of solution of Cr species with 0.001 g of biomass for 2 h. These experiments were done by varying concentrations of adsorbate in solution and then changing the adsorbent dose (0.05, 0.10, 0.25, and 0.50 g $L^{-1}$). $Cr^{VI}$ different concentrations in solutions were 100, 200, 300, 400 and 500 µg $L^{-1}$. After optimizing pH, the concentration of adsorbate, and biosorbent dose, further experiments were done by varying shaking time (5, 10, 20, 30, 40, 50, and 60 min) and temperature (298, 318, 333, 348, and 363 K). The solutions were separated from the biomass by filtering the solutions via the Whatman No. 42 filter paper. MIS-FAAS determined the initial and final $Cr^{VI}$ concentrations in each flask. Finally, the approach was used on actual field samples of industrial effluents from Hyderabad and Jamshoro, Pakistan, at these optimal circumstances. At the appropriate conditions, each experiment was carried out three times.

OPB sample pellets were prepared for FTIR spectroscopic analysis by combining 1:3 OPB and potassium bromide (KBr), which were then pressed into a 13-mm in diameter for 5 minutes. OPB sample pellets were prepared for FTIR spectroscopic analysis by combining 1:3 OPB and potassium bromide (KBr), which were then pressed into a 13-mm diameter for 5 minutes. Before and after $Cr^{VI}$ loading, from 4000 to 400 $cm^{-1}$ of OPB, the pellets were scanned. OPB unloaded and loaded with Using an electric oven at 105°C for one hour, $Cr^{VI}$ was fully dried, and samples were placed on the holders or stubs using double-sided conductive tapes for scanning electron microscopy (SEM) analysis. To eliminate the charge effect, the samples were coated in graphite. SEM analysis of the coated samples was performed using various accelerating voltages and magnifications.

### 2.3.3 Biosorption Capacity

Equation (1) was used to determine the number of sorbates that were adsorbed (in µg or mg) per unit mass of biosorbent ($q_e$):

$$q_e = \frac{(C_i - C_e)}{m} V \quad (1)$$

Where "m" is the dry biomass of peel employed as a biosorbent, "$q_e$" is the biosorption capacity, $C_i$ and $C_e$ are the initial and final concentrations of the sorbate (mg $L^{-1}$), and V is the volume of the solution (L).

## 3. Results and Discussion

Figure 1 a, b, c provides the findings of the physico-chemical characteristics of the composite industrial effluent samples from four distinct industries, including pH, TDS, EC, and BOD. FI, PI, CI, and TFI effluent samples were found to have pH values between 7.00 and 8.60, 6.60 to 6.80, 6.70 to 7.90, and 6.10 to 6.60, respectively. Because various chemicals are used in the cleaning, washing, and polymerization/dying processes in the PI and TFI industries, their pH values are slightly acidic [10]. The pH of the effluent was mildly acidic (5.96 ± 0.09), though higher values (7.16 ± 0.02) were noted. According to Pei et al. [5], the alkaline pH of natural water may affect fish, causing harm to their outside surfaces like their gills, eyes, and skin, as well as making it difficult for them to get rid of metabolic waste. Additionally, the elevated pH of industrial effluents may make other compounds more harmful [5, 19].

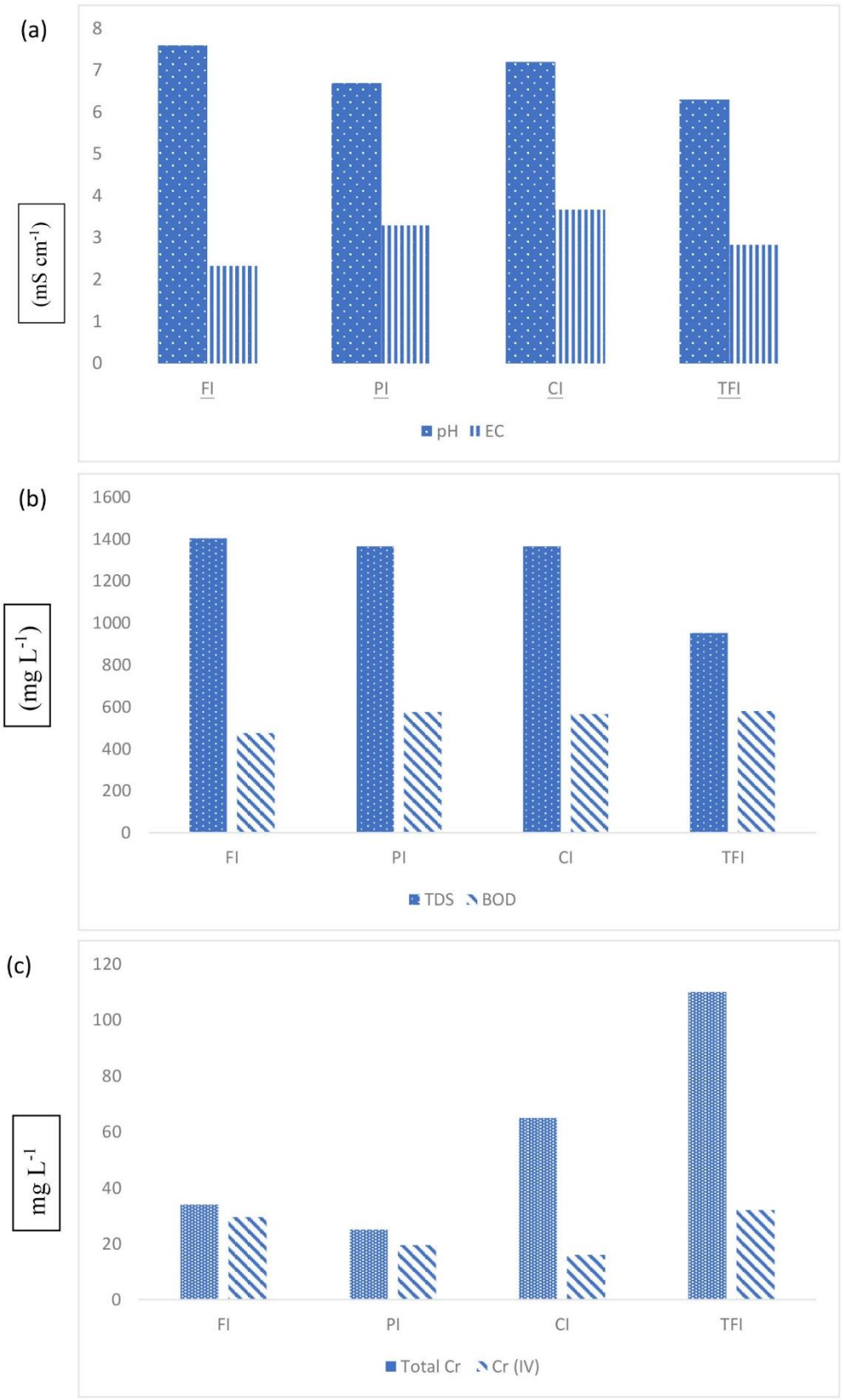


**Figure 1** Physico-chemical parameters of the industrial effluent samples from distinct industries.

TDS levels in effluent samples from FI, PI, CI, and TFI ranged from 951 to 1820, 1348 to 1382, 1345 to 1385, and 450 to 1322, respectively. While the EC of the FI, PI, CI, and TFI effluent samples

under study ranged from 0.87 to 4.01, 3.0 to 3.6, 3.00 to 3.60, and 0.4 to 5.3 mS $cm^{-1}$, respectively. While the EC of the FI, PI, CI, and TFI effluent samples under study ranged from 7.87 to 8.01, 8.0 to 8.6, 6.00 to 7.60, and 8.4 to 9.3 mS $cm^{-1}$, respectively. Based on the concentration, degree of ion dissociation, and temperature, the EC gives information about the dissociated and dissolved chemicals [20]. The relative EC ranges for the effluents of FI, PI, CI, and TFI were 0.87-4.01, 3.00-3.61, 2.88-3.72, and 0.40-5.30 mS $cm^{-1}$. It was discovered that the EC of the industrial effluent types under study exceeded the US-allowed EPA's limits (1.00 mS $cm^{-1}$). It is due to the spilling of oil, grease, ammonia, sulphide, dyes, and waste effluents from TFI, which may result in a decline in the quality of drinking water [5].

The mean BOD values were determined to be 475 ± 61.4, 575 ± 7.10, 565 ± 7.10, and 580 ± 20.0 mg $L^{-1}$ in the effluent samples from FI, PI, CI, and TFI, respectively. This might be due to different chemicals used in textile industries for mercerizing, bleaching/scouring, and yawing which include sodium chlorite, sodium sulphite, NaCl, sodium bisulphate, sodium bicarbonate, formic acid, $H_2SO_4$, vegetable tannins, syntans, resins, sodium formate, polyurethane, fat emulsions, dyes, binders, waxes, pigments, lacquers/formaldehyde, NaOH, sodium phosphate sodium hypochlorite, acids, $H_2O_2$, surfactants, $Cl_2$, and $NaSiO_3$ [21, 22].

The total Cr contents in effluents of FI, PI, CI and TFI varied in the range of 30.0-38.0, 23.0-27.0, 35.0-95.0 and 40.0-180 mg $L^{-1}$, respectively. All of the analyzed industries' effluent samples had total Cr concentrations that exceeded the US EPA threshold of 0.10 mg $L^{-1}$ for total Cr. The total Cr contents showed significantly positive correlation with pH, TDS and EC in effluent samples of FI ($r > 0.60$; $p < 0.20$), whilst strongly negative correlation was observed between total Cr and BOD ($r = -0.61$; $p = 0.20$). The total Cr contents in effluent samples of PI were reversely correlated with pH and TDS ($r > -0.90$; $p > 0.05$), whereas, it has a significant correlation with EC and BOD ($r > 0.80$; $p < 0.10$). However, total Cr levels have a positive correlation with pH and TDS ($r > 0.60$; $p < 0.20$) and a negative correlation with EC and BOD ($r > -0.60$; $p > 0.20$).

### *3.1 Removal of $Cr^{IV}$ from Industrial Effluents by Orange Peel Biosorbent*

#### 3.1.1 FTIR Study of OPB

FTIR spectroscopy is one of the most crucial methods for determining the main functional groups contained in compounds [21, 23]. By comparing the FTIR spectra of OPB before and after $Cr^{VI}$ adsorption, it was feasible to determine the interactions between the functional groups of the orange peel biosorbent (OPB) and $Cr^{VI}$ ions. The unloaded OPB's resulting spectra revealed a broad and powerful peak at 3100-3600 $cm^{-1}$ caused by the overlap of stretching vibrations for -OH and -$NH_2$ (Figure 2). The peak at 2924 $cm^{-1}$ indicates the methyl and methoxy groups' -CH stretching vibration. The peak at 2924 $cm^{-1}$ indicates the methyl and methoxy groups' -CH stretching vibration. A peak at 1741 $cm^{-1}$ is due to carboxylic acid/esters stretching in the -C=O direction. A peak for the -$NH_2$ bending vibration can be found at 1641 $cm^{-1}$. The -$CH_3$ symmetrical deformation mode (scissoring) in the amide group is characterized by a peak at 1381 $cm^{-1}$. The -C-N vibration is indicated by the band at 1246 $cm^{-1}$. The stretching vibrations of carboxylic acids, alcohols, ether, and/or N-H deformation of amines can be attributed to the peaks between 1300 and 1000 $cm^{-1}$ [24].

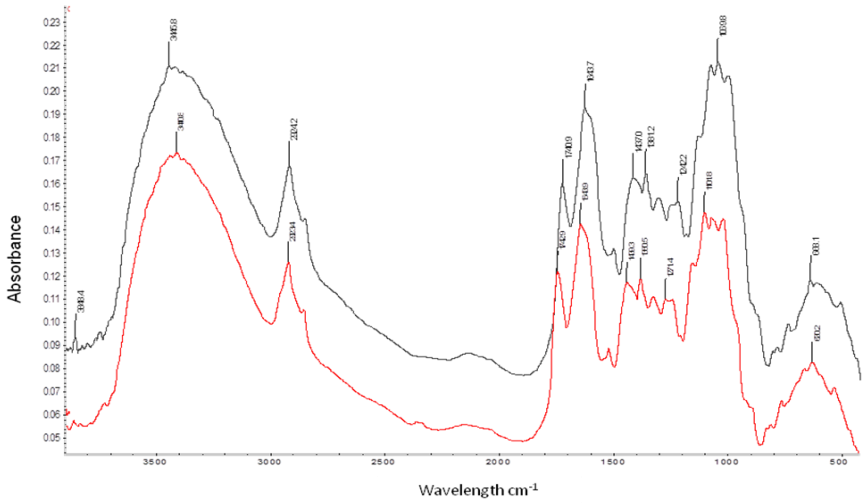


**Figure 2** FTIR spectra of unloaded OPB (black line) and $Cr^{VI}$ loaded OPB (red line).

Peaks in the FTIR spectra of $Cr^{VI}$-loaded OPB are deformed and shifted (Figure 1). At wave number 3446 $cm^{-1}$, which was changed to wave number 3410.8 $cm^{-1}$, a significant difference was seen in the stretching vibration of OH and $NH_2$. Additionally, the -$NH_2$ bending vibration at 1643.7 $cm^{-1}$ wave number was moved to higher frequencies at 1643.9 $cm^{-1}$ (Figure 2). The C-N functional group's FTIR peak moved from 1242 to 1271. In contrast, the peak of -CO was moved from 1069.8 to 1101.8 $cm^{-1}$ by the adsorption of $Cr^{VI}$. Consequently, using FT-IR spectrum analysis, it can be concluded that interactions between biomasses' amine and -CO functional groups allow $Cr^{VI}$ to bind to OPB (the peel of *Citrus aurantium*).

### 3.1.2 SEM Study OPB

Scanning electron microscopy (SEM) was used to examine the surface morphologies of OPB with $Cr^{VI}$ that had been loaded and unloaded and the resulting micrograph is given in Figure 3 a, b. The micrograph (Figure 3a) indicates cavities, pores, and more rough surfaces with several large clusters of mesopores spotted. Due to the high amount of biosorption-ready surface area, this may be the cause of the high biosorption capacity. After $Cr^{VI}$ loading, the change in morphology of OPB that $Cr^{VI}$ is bio-sorbed onto the OPB (Figure 3b).

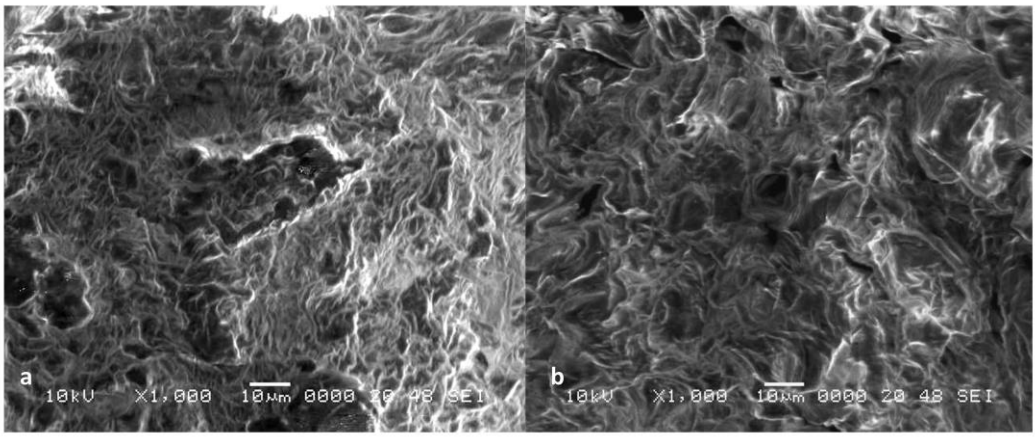


**Figure 3** SEM micrographs of (a) unloaded OPB and (b) $Cr^{VI}$ loaded OPB.

### *3.2 Optimization of Different Parameters for the Removal of $Cr^{VI}$*

#### 3.2.1 Effect of pH

Due to the importance of pH during the biosorption experiment, the impact of pH on the biosorption of $Cr^{VI}$ on OPB was also examined [19, 25]. The interaction between the analyte of interest and the binding sites on the sorbent surface in an aqueous solution was significantly impacted by the pH variation. Between pH 2 and 9, at a given concentration of $Cr^{VI}$ (0.25 mg $L^{-1}$), we looked at the effects of pH, contact time (20 minutes), biosorbent dosage (0.01 g $L^{-1}$), and temperature on the binding of $Cr^{VI}$ on the surface of OPB (298 K) as shown in Figure 4. In the pH range of 2 to 7, it was discovered that the biosorption was more than 94%. This is because, $Cr^{VI}$ exists in dichromate, form either in $K_2Cr_2O_7$ or anionic $Cr_2O_7^{-2}$ at pH 2.0 to 7.0. However, the maximum biosorption ($q_e$ max = 47.0-48.0 mg $g^{-1}$) was achieved at pH 5.0-7.0. Thus, pH 7.0 was selected for further experiments.

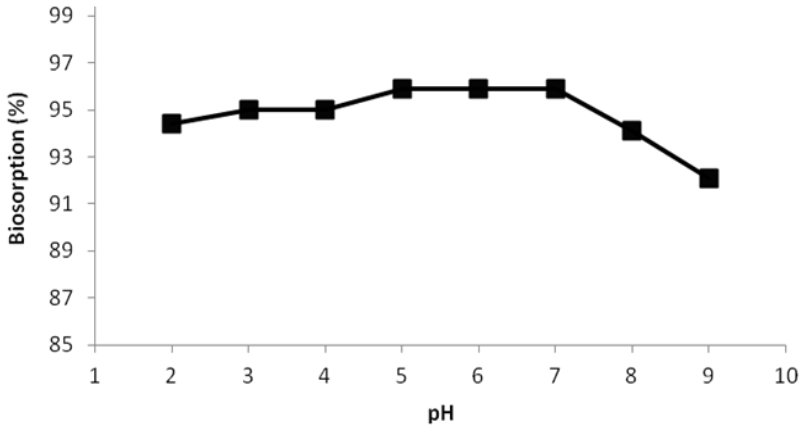


**Figure 4** Effect of pH of the biosorption of $Cr^{VI}$ by OPB at $Cr^{VI}$ concentration 0.25 mg $L^{-1}$; contact time 20 minutes; adsorbent dosage 0.1 g $L^{-1}$ and temperature 298 K.

#### 3.2.2 Effect of Concentration

The effect of $Cr^{VI}$ concentration on the investigation of the quantitative biosorption, with all parameters at constant values from 0.05-1.0 mg $L^{-1}$ (Figure 5). According to the results, the % biosorption of $Cr^{VI}$ was steady >0.25 mg $L^{-1}$, but after that point, a gradual decline in the % biosorption was observed (Figure 5). This might be due to the limited active sites of the biosorbent for the removal of $Cr^{VI}$. As a result, 0.25 mg $L^{-1}$ of $Cr^{VI}$ concentration was selected as the quantitative concentration for additional tests.

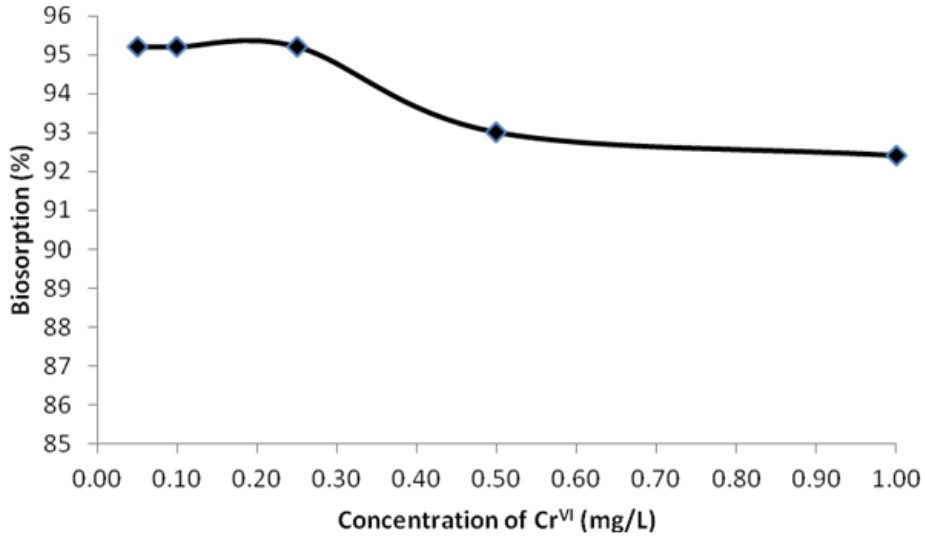


**Figure 5** Effect of $Cr^{VI}$ concentration (mg $L^{-1}$) by OPB at contact time 20 minutes; adsorbent dosage 0.1 g $L^{-1}$; temperature 298 K and pH 7.0.

3.2.3 Effect of Dosage

When the $Cr^{VI}$ concentration was 0.25 mg $L^{-1}$, the contact time was 20 minutes, the temperature was 298 K, and the pH was 7.0, the impact of biosorbent (OPB) dosage on the % of $Cr^{VI}$ biosorption (Figure 6). Gradually increasing the OPB dosage from 0.05 to 0.10 g $L^{-1}$ (Figure 6) has increased in the % biosorption (50.0 to 95.5%). With the increased dosage of OPB, there was no discernible increase in % biosorption. As a result, the dosage of 0.10 g $L^{-1}$ OPB has been chosen for the quantitative elimination of $Cr^{VI}$.

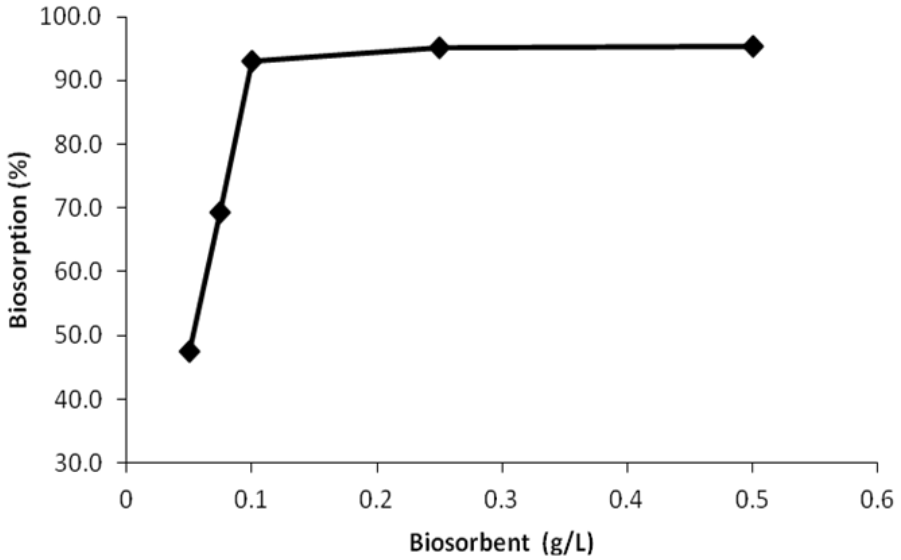


**Figure 6** Effect of dosage of biosorbent for the removal of $Cr^{VI}$ by OPB at $Cr^{VI}$ concentration 0.25 mg $L^{-1}$; contact time 20 minutes; temperature 298 K and pH 7.0.

3.2.4 Effect of Contact Time and Temperature

The effect of contact time for the quantitative % biosorption of $Cr^{VI}$ has been checked from 5.0 to 60 min (Figure 7). At the initial stage, the biosorption rate of $Cr^{VI}$ was very rapid as over 80% of $Cr^{VI}$ was absorbed at both 5.0 and 10 min for OPB. Later on, near the 20-minute equilibrium point, it started to slow down the percent of biosorption. Following that, there was no discernible change in the % of $Cr^{VI}$ biosorption. In order to determine the quantitative % biosorption under equilibrium conditions, 20 min contact duration has been chosen. Similar research has been done on the impact of temperature for the quantitative % biosorption of $Cr^{VI}$ from 298 to 363 K at the optimal values of other parameters (Figure 7). According to reports, when the temperature rises, the % of $Cr^{VI}$ absorbed by the OPB will gradually decline (Figure 7). $Cr^{VI}$ elimination from complicated aqueous solution at ambient temperature is thus best accomplished by the proposed OPB (298-303 K).

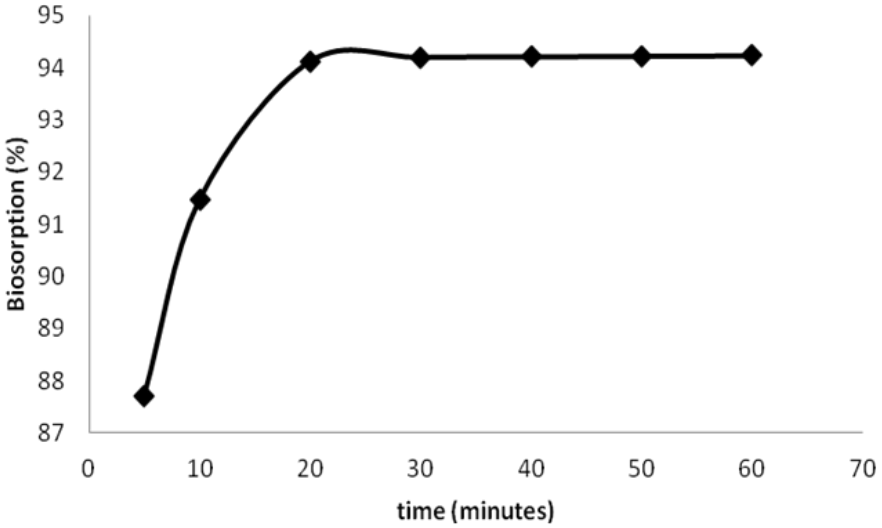


**Figure 7** Effect of contact time for the removal of $Cr^{VI}$ by OPB at $Cr^{VI}$ concentration 0.25 mg $L^{-1}$ adsorbent dosage 0.01 g $L^{-1}$ temperature 298 K and pH 7.0.

### *3.3 Isothermal Study*

The Langmuir, Freundlich, and Dubinin-Radushkevich isotherm models have all been used to describe the biosorption of $Cr^{VI}$ at equilibrium conditions. The Langmuir theory's fundamental premise is that sorption occurs at particular homogenous spots within the sorbent [26, 27]. The outcomes of a plot of Ce/qe vs. Ce shown as a straight line with a slope of 1/Q and an intercept of 1/Qb are shown in Table 2. The biosorption of $Cr^{VI}$ ions onto biosorbent material was highly linear in the Langmuir model. The magnitude of Q was found to be 0.298-0.308 mmol $g^{-1}$ (47.0-48.0 mg $g^{-1}$) at 298 K. The value of b was noted from 4.70 to 6.30 × $10^{-2}$ L $mol^{-1}$. $Cr^{VI}$ strongly bonds to the biosorbent material at 298 K is also implied by a high value for "b".

**Table 2** Langmiur, Freundlich and D-R characteristic constants for $Cr^{VI}$ biosorption onto OPB.

| Isotherm model | Parameters | Unit | 298 K |
|---|---|---|---|
| Langmiur | Q | (mmol $g^{-1}$) | 0.303 ± 0.01 |
| | B | (L $mol^{-1}$) | $5.50 \times 10^{-2}$ ± 0.88 |
| | $R_L$ | | 0.124-0.987 |
| | $R^2$ | | 0.987 |
| Freundlich | $C_m$ | (mmol $g^{-1}$) | 1.120 ± 0.22 |
| | N | | 0.810 ± 0.25 |
| | $R^2$ | | 0.991 |
| D-R | $X_m$ | (mmol $g^{-1}$) | 12.2 ± 0.15 |
| | E | (kJ $mol^{-1}$) | 8.77 ± 0.18 |
| | $R^2$ | | 0.992 |

A dimensionless characteristic parameter ($R_L$) has been estimated from the value of b. The $R_L$ was found in the range of 0.124 to 0.987 by using the relationship:

$$R_L = \frac{1}{1 + bC_i} \quad (2)$$

Where, b is the Langmuir constant and $C_i$ is the initial concentration. The calculated values of $R_L$ have predicted the favorable biosorption of $Cr^{VI}$ ions onto OPB at 298 K. The $R_L$ between 0 and 1, demonstrated that the biosorption process was quite favorable at 298 K.

The intercept and slope of the linear plot of lnqe vs. lnCe are used to calculate the Freundlich constants Cm and 1/n, respectively. The 1/n ratio was in the range of 0 and 1, indicating that the conditions for the biosorption of the understudy biosorbent material were good (Table 2). However, as the $R^2$ value was found to be >0.99, the relationship between the quantities of biosorbed $Cr^{VI}$ ions and their equilibrium concentration in the solution was determined to be consistent with the Freundlich model.

The potential biosorption process mechanism can be hypothesized. One mole of solute was found to have a free energy of transfer (E) of 8.60 to 9.00 kJ $mol^{-1}$ from the solution to the surface of the biosorbent material using the equation $E = 1/\sqrt{-2\beta}$. The obtained E values demonstrated that the biosorption process involves chemical ion exchange, whereas E 8 kJ $mol^{-1}$ demonstrated that physical sorption is also involved [28, 29]. Therefore, the sorption of $Cr^{VI}$ onto OPB may be a combination of physical processes according to biosorption energy. All three isotherms provided strong correlation coefficients and a good match to the experimental data (Table 2). The ability of all three isotherms to be used for the biosorption of arsenic demonstrates the viability of heterogeneous energy distribution of active sites on the OPB surface as well as monolayer sorption.

### *3.4 Kinetic Study*

The workings of the adsorbate-biosorbent system and its response time can be better understood by using kinetic models. The pseudo-first-order and pseudo-second-order models were assessed in order to understand the experimental findings in order to determine the kinetic

configuration that governs the biosorption phenomena [28, 30]. The results of the experiments were also tested using the pseudo-second-order kinetic model. With chemical sorption acting as the rate-controlling step, this model is more likely to predict the kinetic behavior of biosorption [31]. The pseudo-second-order rate constant, $k_2$, and $q_e$, was calculated using the slope and intercept plots of t/qt vs. t (Table 3). The estimated and observed $q_e$ values coincide, and the plots exhibit good linearity with an $R^2$ of better than 0.96.

**Table 3** Kinetic parameters obtained from pseudo-first-order and pseudo-second-order for $Cr^{VI}$ biosorption onto OPB.

| Order of reaction | Parameters | Unit | 298 K |
|---|---|---|---|
| | $q_e$, exp | (μmol $g^{-1}$) | 220 ± 2.50 |
| pseudo-first-order | $k_1$ | (1 min) | $9.60 \times 10^{-2}$ |
| | $q_e$ | (μmol $g^{-1}$) | 10.2 |
| | $R^2$ | | 0.957 |
| pseudo-second-order | $k_2$ | (g μmol$^{-1}$ min$^{-1}$) | $1.70 \times 10^{-2}$ |
| | $q_e$ | (μmol $g^{-1}$) | 132 |
| | $R^2$ | | 0.964 |

### *3.5 Thermodynamic Study*

The thermodynamic characteristics of the biosorption of $Cr^{VI}$ onto OPB were calculated using equations 1 and 2, including enthalpy change (ΔH°), Gibbs free energy change (ΔG°), and entropy change (ΔS°). The Gibbs free energy measures how spontaneously the biosorption process occurs, and a higher negative value suggests more advantageous sorption from an energetic standpoint [31]. At all study temperatures, the value of ΔG° was negative. The ΔG° values are unchanged until 318 K, after which they slightly decline (Table 4). Enthalpy, or heat, of biosorption for physical biosorption ranges from 0.5 to 5 kcal mol$^{-1}$ [25]. Additionally, the positive value of So (Table 4) denotes the likelihood of advantageous biosorption.

**Table 4** Thermodynamic parameters for $Cr^{VI}$ biosorption onto OPB.

| Thermodynamic Parameter | Equation | Plot | Values |
|---|---|---|---|
| Change in free energy (kJ mol$^{-1}$) | $\Delta G^\circ = -RT\ln K_a$ | | |
| | Temperature range | 298 K | -30.2 |
| | | 318 K | -30.2 |
| | | 333 K | -29.3 |
| Change in enthalpy (kJ mol$^{-1}$) | $\ln nK_a = \frac{\Delta S^\circ}{R} - \frac{\Delta H^\circ}{RT}$ | lnK vs.1/T | 0.002 |
| Change entropy (kJ mol$^{-1}$ K$^{-1}$) | | | 0.015 |

### *3.6 Desorption and Regeneration Studies*

HCl, $HNO_3$, and NaOH were used in varying quantities to desorb the biosorbed $Cr^{VI}$ ions from the OPB. (Table 5). It was shown that 1.0 mol $L^{-1}$ HCL desorbed more than >93% of $Cr^{VI}$, whereas 1.0 mol $L^{-1}$ $HNO_3$ and NaOH recovered roughly 91.4 and 89.5% of $Cr^{VI}$, respectively. For the following studies,

biosorbed $Cr^{VI}$ on OPB was dissolved in 10 mL of 1.0 mol $L^{-1}$ HCl. After ten studies, it was found that the biosorbent material's capacity was essentially constant (deviation of 1-2%); hence, many biosorbent material uses were deemed sufficient.

**Table 5** Influence of different eluents of the % desorption of $Cr^{VI}$ from OPB.

| Eluent | Concentration (mol $L^{-1}$) | % Recovery |
|---|---|---|
| HCl | 0.1 | 68.7 ± 0.75 |
| | 0.5 | 79.5 ± 0.94 |
| | 1.0 | 93.4 ± 0.90 |
| $HNO_3$ | 0.1 | 55.4 ± 0.85 |
| | 0.5 | 65.4 ± 0.80 |
| | 1.0 | 91.4 ± 0.70 |
| NaOH | 0.1 | 45.7 ± 0.98 |
| | 0.5 | 58.7 ± 0.78 |
| | 1.0 | 89.5 ± 0.74 |

### *3.7 Application on Industrial Effluents*

This study has shown that OPB has the potential to remove $Cr^{VI}$ from the industrial effluents of several Hyderabadi and Jamshoro enterprises. The OPB's most alluring feature is that it can be collected as waste in significant amounts from juice factories and retailers around the nation. Through a series of tests, the OPB proved that at pH 7, >10.0 mg $L^{-1}$ of $Cr^{VI}$ that was present in the industrial effluents of various industries could be removed (Table 6). It might, therefore, be suggested for the effective removal of $Cr^{VI}$ from the effluent of various industries.

**Table 6** Analytical data of $Cr^{VI}$ concentration in effluent samples of different industries before and after biosorption.

| Industry | Before biosorption | After biosorption |
|---|---|---|
| | $Cr^{VI}$ (mg $L^{-1}$) | |
| Food Industry (n = 30) | 29.5 ± 6.50 | 27.8 ± 5.40 |
| Plastic Industry (n = 30) | 19.5 ± 0.50 | 18.4 ± 0.28 |
| Chemical Industry (n = 30) | 16.0 ± 7.00 | 14.9 ± 5.80 |
| Textile and Fabrics Industry (n = 30) | 32.0 ± 9.40.0 | 30.0 ± 8.50 |

## 4. Conclusion

It has been determined that the levels of EC, TDS, and BOD in effluent samples from four industries were much higher than the US EPA legal limit. Industrial wastewater samples from the textile industry exhibited increased levels of total Cr that were 400-1800 times greater than the amount allowed by US EPA regulation. In effluent samples from FI, CI, and TFI, the amounts of total Cr were shown to have a significant linear association coefficient with pH, TDS, EC, and BOD ($p < 0.01$). 1.0 mol $L^{-1}$ HCl desorbed the $Cr^{VI}$ from OPB than 1.0 mol $L^{-1}$ $HNO_3$ or NaOH. The interactions between $Cr^{VI}$ and the functional groups on the OPB surface were studied using FTIR and SEM. The

biosorption of $Cr^{VI}$ onto OPB was demonstrated by a kinetic examination of the equilibrium data, which followed the pseudo-second-order kinetic model well. Based on these findings, it can be said that OPB, which has a high biosorption capability, is a viable alternative for removing $Cr^{VI}$ from aqueous solutions and is also readily available and environmentally acceptable.

**Author Contributions**

Muhammad Waris: Conceptualization, writing – original draft, writing – review and editing. Muhammad Kashif Channa: Software, writing – review and editing. Sultana Rahman: Methodology, writing – review and editing. Ali Bahar Shahani: Conceptualization, review and editing. All authors have read and approved the published version of the manuscript.

**Competing Interests**

The authors have declared that no competing interests exist.

**References**

1. Kotaś J, Stasicka ZJ. Chromium occurrence in the environment and methods of its speciation. Environ Pollut. 2000; 107: 263-283.
2. Cheung KH, Gu JD. Mechanism of hexavalent chromium detoxification by microorganisms and bioremediation application potential: A review. nt Biodeterior Biodegrad. 2007; 59: 8-15.
3. Matos GD, dos Reis EB, Costa AC, Ferreira SL. Speciation of chromium in river water samples contaminated with leather effluents by flame atomic absorption spectrometry after separation/preconcentration by cloud point extraction. Microchem J. 2009; 92: 135-139.
4. Krishna PG, Gladis JM, Rambabu U, Rao TP, Naidu GR. Preconcentrative separation of chromium (VI) species from chromium (III) by coprecipitation of its ethyl xanthate complex onto naphthalene. Talanta. 2004; 63: 541-546.
5. Pei Y, Yang Y, Chen L, Yang Y, Song L. Remediation of chromium-contaminated soil in semi-arid areas by combined chemical reduction and stabilization. Environ Pollut Bioavailab. 2023; 35: 2157332.
6. Narin I, Kars A, Soylak M. A novel solid phase extraction procedure on amberlite XAD-1180 for speciation of Cr (III), Cr (VI) and total chromium in environmental and pharmaceutical samples. J Hazard Mater. 2008; 150: 453-458.
7. Dhal B, Thatoi HN, Das NN, Pandey BD. Chemical and microbial remediation of hexavalent chromium from contaminated soil and mining/metallurgical solid waste: A review. J Hazard Mater. 2013; 250: 272-291.
8. Jakubus M. Changes in lead and chromium contents in sewage sludge evaluated using both single extractants and sequential method. Environ Pollut Bioavailab. 2020; 32: 87-99.
9. Lovelyn NU, Egbulezu AV, Chudi OP. Assessment of heavy metal pollution of effluents from three food industries within Onitsha in Anambra State, Nigeria. Int J Environ Monit Anal. 2014; 2: 259-265.
10. Ado A, Gumel SM, Garba J. Industrial effluents as major source of water pollution in Nigeria: An overview. Am J Chem Appl. 2014; 1: 45-50.

11. Kanu I, Achi OK. Industrial effluents and their impact on water quality of receiving rivers in Nigeria. J Appl Technol Environ Sanit. 2011; 1: 75-86.
12. Fang Z, Wang Q, Zhang C, Li S, Li S, Wang X, et al. Effects of Cr6+ stress on chromium chemical speciation distribution and bacterial community structure in the Coix lacryma-jobi L. constructed wetlands. Environ Pollut Bioavailab. 2022; 34: 433-445.
13. Pehlivan E, Cetin S. Sorption of Cr (VI) ions on two Lewatit-anion exchange resins and their quantitative determination using UV-visible spectrophotometer. J Hazard Mater. 2009; 163: 448-453.
14. Qureshi I, Memon S, Yilmaz M. Estimation of chromium (VI) sorption efficiency of novel regenerable p-tert-butylcalix [8] areneoctamide impregnated amberlite resin. J Hazard Mater. 2009; 164: 675-682.
15. Gao Y, Zhao F, Zhao Y, Sun Y, Zhang D, Yuan L, et al. Enhancement of chromium contaminated soil remediation by ferrous sulfate with the addition of biogas residue. Environ Prog Sustain Energy. 2022; 41: e13816.
16. Li X, Tang Y, Cao X, Lu D, Luo F, Shao W. Preparation and evaluation of orange peel cellulose adsorbents for effective removal of cadmium, zinc, cobalt and nickel. Colloids Surf A Physicochem Eng Asp. 2008; 317: 512-521.
17. Elci L, Kartal AA, Soylak M. Solid phase extraction method for the determination of iron, lead and chromium by atomic absorption spectrometry using Amberite XAD-2000 column in various water samples. J Hazard Mater. 2008; 153: 454-461.
18. Waris M, Kazi TG, Baig JA. Evaluation and speciation of cobalt, copper, and zinc in saline soil by microwave-assisted single extraction. Environ Prog Sustain Energy. 2021; 40: e13610.
19. Patyal V, Jaspal D, Khare K. Performance enhancement of constructed wetlands for wastewater remediation by modifications and integration of technologies: A review. Environ Prog Sustain Energy. 2023; 42: e13951.
20. Rendina A, Josefina Barros M, Fabrizio de Iorio A. Changes in the speciation, partitioning and phytoavailability of chromium induced by organic soil amendments. Chem Spec Bioavailab. 2011; 23: 53-60.
21. Emoyan OO, Akporhonor EE, Akpoborie IA. Environmental risk assessment of River Ijana, Ekpan, Delta State Nigeria. Chem Spec Bioavailab. 2008; 20: 23-32.
22. Sahmoune MN, Louhab K, Boukhiar A. Advanced biosorbents materials for removal of chromium from water and wastewaters. Environ Prog Sustain Energy. 2011; 30: 284-293.
23. Liu Y, Xu Z, Hu X, Zhang N, Chen T, Ding Z. Sorption of Pb(II) and Cu(II) on the colloid of black soil, red soil and fine powder kaolinite: Effects of pH, ionic strength and organic matter. Environ Pollut Bioavailab. 2019; 31: 85-93.
24. Zewde D, Geremew B. Removal of Congo red using Vernonia amygdalina leaf powder: Optimization, isotherms, kinetics, and thermodynamics studies. Environ Pollut Bioavailab. 2022; 34: 88-101.
25. Anggayasti WL, Salamah LN, Rizkymaris A, Yamamoto T, Kurniawan A. The role of ion charge density and solubility in the biosorption of heavy metals by natural biofilm matrix of polluted freshwater: The cases of Mg(II), Cr(VI), and Cu(II). Environ Pollut Bioavailab. 2023; 35: 2220571.
26. Kundu S, Gupta AK. Arsenic adsorption onto iron oxide-coated cement (IOCC): Regression analysis of equilibrium data with several isotherm models and their optimization. Chem Eng J. 2006; 122: 93-106.

27. Sharma P, Goyal P, Srivastava S. Biosorption of trivalent and hexavalent chromium from aqueous systems using shelled moringa oleifera seeds. Chem Spec Bioavailab. 2007; 19: 175-182.
28. Baig JA, Hol A, Akdogan A, Kartal AA, Divrikli U, Kazi TG, et al. A novel strategy for chromium speciation at ultra-trace level by microsample injection flame atomic absorption spectrophotometry. J Anal At Spectrom. 2012; 27: 1509-1517.
29. Panhwar AH, Kazi TG, Afridi HI, Arain SA, Arain MS, Brahaman KD, et al. Correlation of cadmium and aluminum in blood samples of kidney disorder patients with drinking water and tobacco smoking: Related health risk. Environ Geochem Health. 2016; 38: 265-274.
30. Razavi M, Yousefi Kebria D, Ebrahimi A. Microbial fuel cell-enhanced electrokinetic process for remediation of chromium from marine sediments. Environ Prog Sustain Energy. 2021; 40: e13469.
31. Baig JA, Kazi TG, Shah AQ, Arain MB, Afridi HI, Khan S, et al. Evaluating the accumulation of arsenic in maize (Zea mays L.) plants from its growing media by cloud point extraction. Food Chem Toxicol. 2010; 48: 3051-3057.